THE JOURNAL OF BIOLOGICAL CHEMISTRY
Vol. 278, No. 47, Issue of November 21, pp. 46840–46846, 2003
Printed in U.S.A.

F_0F_1-ATPase/Synthase Is Geared to the Synthesis Mode by Conformational Rearrangement of ε Subunit in Response to Proton Motive Force and ADP/ATP Balance*

Received for publication, July 4, 2003, and in revised form, July 24, 2003
Published, JBC Papers in Press, July 24, 2003, DOI 10.1074/jbc.M307165200

Toshiharu Suzuki‡§, Tomoe Murakami‡, Ryota Iino‡§, Junko Suzuki‡, Sakurako Ono§, Yasuo Shirakihara¶, and Masasuke Yoshida‡§‖

From the ‡ATP System Project, Exploratory Research for Advanced Technology (ERATO), Japan Science and Technology Corporation (JST), Nagatsuta 5800-2, Yokohama 226-0026, Japan, the §Chemical Resources Laboratory, Tokyo Institute of Technology, Nagatsuta 4259, Yokohama 226-8503, Japan, and the ¶National Institute of Genetics, Mishima, Shizuoka 411-8540, Japan

The ε subunit in F_0F_1-ATPase/synthase undergoes drastic conformational rearrangement, which involves the transition of two C-terminal helices between a hairpin "down"-state and an extended "up"-state, and the enzyme with the up-fixed ε cannot catalyze ATP hydrolysis but can catalyze ATP synthesis (Tsunoda, S. P., Rodgers, A. J. W., Aggeler, R., Wilce, M. C. J., Yoshida, M., and Capaldi, R. A. (2001) *Proc. Natl. Acad. Sci. U. S. A.* 98, 6560–6564). Here, using cross-linking between introduced cysteine residues as a probe, we have investigated the causes of the transition. Our findings are as follows. (i) In the up-state, the two helices of ε are fully extended to insert the C terminus into a deeper position in the central cavity of F_1 than was thought previously. (ii) Without a nucleotide, ε is in the up-state. ATP induces the transition to the down-state, and ADP counteracts the action of ATP. (iii) Conversely, the enzyme with the down-state ε can bind an ATP analogue, 2′,3′-*O*-(2,4,6-trinitrophenyl)-ATP, much faster than the enzyme with the up-state ε. (iv) Proton motive force stabilizes the up-state. Thus, responding to the increase of proton motive force and ADP, F_0F_1-ATPase/synthase would transform the ε subunit into the up-state conformation and change gear to the mode for ATP synthesis.

F_0F_1-ATPase/synthase (F_0F_1)[1] catalyzes ATP synthesis/hydrolysis coupled with a transmembrane H^+(proton)-translocation in bacteria, chloroplasts, and mitochondria (1–5). The enzyme is composed of two portions, *i.e.* a water-soluble F_1, which has catalytic sites for ATP synthesis/hydrolysis, and a membrane-integrated F_0, which mediates proton translocation. The bacterial enzyme has the simplest subunit structure, $\alpha_3\beta_3\gamma_1\delta_1\epsilon_1$ for F_1 and $a_1b_2c_{10-11(?)}$ for F_0. F_1 is reversibly detached from F_0 and is by itself a rotary motor driven by ATP hydrolysis (6–8) in which a central stalk made of γ and ε subunits rotates relative to the surrounding $\alpha_3\beta_3$ hexamer ring where hydrolysis occurs (9, 10). The remaining F_0 portion in the membrane acts as a proton channel that mediates passive proton translocation across the membrane (11).

The ε subunit is known as an endogenous inhibitor of ATPase activity of F_1 and F_0F_1 (12, 13). Structures of the isolated ε from *Escherichia coli*, as determined by x-ray crystallography (14) and NMR spectroscopy (15, 16), show that ε consists of two distinct domains. A C-terminal helical hairpin domain of ~50 residues lies on an N-terminal 10-stranded β sandwich domain of ~80 residues (Fig. 1*A*). The δ subunit (equivalent to the bacterial ε subunit) in the crystal structure of bovine mitochondrial F_1 also has a two-domain conformation that is very similar to that of the isolated bacterial ε and is associated with the "bottom" globular part of the γ subunit (we refer to this conformational state of ε as the "down"-state hereafter) (Fig. 1*B*) (17). However, the down-state ε does not exhibit an inhibitory effect on ATPase activity because, when down-state conformation is locked by cross-linking between the two domains, the inhibitory effect of ε is lost, and apparent activation of ATP hydrolysis is observed (18, 19). Actually, in the structure of mitochondrial F_1, the δ subunit does not have any contact with the $\alpha_3\beta_3$ (Fig. 1*B*). Another conformation of ε was suggested from observations that the residue (εSer^{108}, *E. coli* numbering) in the C-terminal domain of the *E. coli* ε subunit has interactions with the residues (βGlu^{381}) in the "DELSEED" region of the β subunit (and the homologous region of the α subunit) (9, 20–22). Also, it was shown that positive residues in the C-terminal domain of the ε subunit of thermophilic F_1 from thermophilic *Bacillus* PS3 would make electrostatic interaction with the DELSEED region of the β subunit (23). The dynamic and flexible nature of the ε subunit has been also reported for chloroplast F_0F_1 (24). In accordance with these biochemical results, a new conformation of ε was found in the crystal structure of the complex of truncated-γ (γ′) and ε of *E. coli* F_1 (Fig. 1*C*) (25). In this γ′ε complex, a helical hairpin in the previous structures of ε is opened, and the helices are lifted up. Such a location of the ε subunit could be an obstacle for the rotation of the γ subunit and, indeed, F_0F_1, with the ε locked to this lifted-up conformation by γ-ε cross-linking, did not show ATP hydrolysis activity. Interestingly, however, the activity of ATP synthesis of this cross-linked enzyme was fully retained (26). Thus, it has been established that ε can adopt at least two conformational states, *i.e.* the down-state in which C-terminal helices form a hairpin and the up-state in which the helices are extended. Only the ε subunit in the up-state can exert an inhibitory effect on ATPase activity.

* This work was supported in part by Human Frontiers Science Program Organization Grant RG15/1998-M. The costs of publication of this article were defrayed in part by the payment of page charges. This article must therefore be hereby marked "*advertisement*" in accordance with 18 U.S.C. Section 1734 solely to indicate this fact.

‖ To whom all correspondence should be addressed. Tel.: 81-45-924-5233; Fax: 81-45-924-5277; E-mail: myoshida@res.titech.ac.jp.

[1] The abbreviations used are: F_0F_1, the general name of F_0F_1-ATPase/synthase or the particular F_0F_1 from thermophilic *Bacillus* PS3, per context; F_1, the general name of F_1-ATPase or the particular F_1 from thermophilic *Bacillus* PS3, per context; DTNB, 5,5′-dithiobis-(2-nitro)benzoic acid; DTT, dithiothreitol; FCCP, carbonyl cyanide *p*-trifluoromethoxyphenylhydrazone; TNP-AT(D)P, 2′,3′-*O*-(2,4,6-trinitrophenyl)-AT(D)P.

Although the importance of the conformational transition of ε has been thus recognized, the following critical questions on this transition remain unanswered. (i) What is the actual up-state conformation of ε in native F_0F_1? The present knowledge on the up-state conformation of ε is largely based on the crystal structure of the γ′ε complex. However, it is obvious that truncated γ′ imposes an artificial constraint on the conformation of ε (as well as γ) in the γ′ε structure. Indeed, if the extreme C-terminal helix of ε were to have the same conformation as in the γ′ε, it would clash sterically with the closest β subunit. In addition, in the model reconstituted from the $\alpha_3\beta_3\gamma$ part of the mitochondrial F_1 structure and the γ′ε structure, εSer^{108} in the γ′ε is apparently too far from βGlu^{381} to account for efficient cross-linking (Fig. 1*C*). In a 4.4-Å resolution electron density map of *E. coli* F_1, the first α helix of the ε subunit in the extended conformation was barely seen as continuous density, but the second α helix was unable to be traced (27). Therefore, the conformation and arrangement of the up-state ε in intact F_0F_1 is yet unclear. (ii) What is the effect of ATP and ADP on the conformational transition of ε in F_0F_1? In *E. coli* F_1, depending on whether the added nucleotide is ATP or ADP, the same residue of the εE108C changes the cross-linking partner subunit; ε-α in Mg^{2+} + ATP state (in the presence of $MgCl_2$ + 5′-adenylyl-β,γ-imidodiphosphate) and ε-β in the Mg^{2+} + ADP state (20, 28). However, the individual roles of ATP and ADP were not obvious for F_1 from thermophilic *Bacillus* PS3 in our previous paper (19). The distinct role of ATP and ADP in the conformational transition of the ε must be clarified. (iii) Do the enzyme with the up-state ε and the enzyme with the down-state ε have different affinities to ATP and ADP? If ATP and ADP have different effects on the conformational transition of ε, binding affinity to ATP and ADP, conversely, might be different between the enzyme with the up-state ε and the enzyme with the down-state ε. (iv) Does the proton motive force affect the transition of ε? Because the enzyme with the up-state ε can apparently catalyze ATP synthesis but not ATP hydrolysis, the enzyme with the up-state ε can be regarded as the enzyme species geared to the ATP synthesis mode. If so, it is natural to expect that proton motive force would facilitate the down-to-up transition of the ε subunit. To address these questions, we generated a new set of F_0F_1 mutants from thermophilic *Bacillus* PS3 that enabled us to detect and fix the down- and up-states of ε in the working enzyme.

EXPERIMENTAL PROCEDURES

Preparation of the Enzymes—Plasmids for three F_0F_1 mutants, $\gamma_c\epsilon_c$-F_0F_1 (γS3C, εCys^{134}), $\gamma_c\epsilon_{cc}$-F_0F_1 (γS3C, εA85C, εCys^{134}), and ϵ_{cc}-F_0F_1 (εA85C, εCys^{134}), were constructed from the plasmid pTR19-ASDS (29) by the Mega-primer method (30). Sequences of the regions amplified by PCR were verified by nucleotide sequencing. These plasmids were used for transformation of an *E. coli* strain DK8 (bglR, thi-1, rel-1, HfrPO1, Δ(*unc*B-*uncC*), ilv:Tn10) that lacked whole F_0F_1 genes. F_1 ($\alpha_3\beta_3\gamma\delta\epsilon$ complex) of thermophilic *Bacillus* strain PS3 was purified as follows. *E. coli* cells (DK8/pTR19-ASDS) expressing thermophilic F_0F_1 were disrupted in PA3-buffer (10 mM HEPES/KOH, pH 7.5, 5 mM $MgCl_2$, and 10% glycerol) (29), and the cytosol fraction was obtained by removing a membrane fraction with centrifugation (150,000 × *g* for 20 min). The supernatant was incubated at 67 °C for 15 min, and aggregated *E. coli* proteins were removed by centrifugation (150,000 × *g* for 20 min). A yellow supernatant was supplemented with 2 volumes of 20 mM KPi buffer (pH 7.5) containing 100 mM KCl and 50 mM imidazole and applied on a nickel-nitrilotriacetic acid Superflow column (Qiagen, Hilden, Germany) equilibrated with the same buffer. After washing the column with 10 volumes of the buffer, F_1 was eluted with 20 mM KPi buffer, pH 7.5, containing 100 mM KCl and 200 mM imidazole, and DTT (final concentration, 50 mM) was added to the eluted fraction. After incubation for 60 min at 25 °C, ammonium sulfate was added to the solution (final concentration, 1 M), and the solution was applied to a phenyl-Toyopearl 650 M column (Tosoh, Tokyo, Japan) equilibrated with 20 mM KPi buffer, pH 7.5, containing 0.5 mM EDTA and 1 M ammonium sulfate. The column was washed with 20 volumes of 100 mM KPi buffer, pH 7.5, containing 4 mM EDTA and 1 M ammonium sulfate to remove endogenously bound nucleotides, and a linear reverse gradient of ammonium sulfate (1–0 M) was applied. Fractions containing F_1 were collected, precipitated with ammonium sulfate, and further purified with a Superdex 200HR column (Amersham Biosciences) in 20 mM HEPES/KOH buffer, pH 7.5, containing 100 mM KCl. The purified protein was frozen with liquid N_2 and stored at −80 °C until use. The purified $\gamma_c\epsilon_c$-F_1, $\gamma_c\epsilon_{cc}$-F_1 and ϵ_{cc}-F_1 contained 0.096 ± 0.01, 0.18 ± 0.02, and 0.18 ± 0.02 mol of ADP per mol of F_1, respectively.

Assays of Membrane Vesicles—Inverted membrane vesicles from *E. coli* cells expressing thermophilic F_0F_1 were prepared by the procedures described previously (29) except for a modification in which 5 mM DTT was supplemented to the cell extract just after disruption of the cells. The thermophilic F_0F_1 used in this work has a histidine tag of 10 residues at the N terminus of the β subunit. Prior to use, the membrane vesicles were washed twice with PA3 buffer to remove DTT. ATPase activities of the membrane vesicles containing the F_0F_1 mutants were inactivated by *N,N*′-dicyclohexylcarbodiimide down to < 20% of the initial activities, which were almost the same as in the case of the wild-type (15–20%). ATP-driven proton pump activity of membrane vesicles was assayed with fluorescence quenching of 9-amino-6-chloro-2-methoxyacridine at 40 °C in PA4 buffer (10 mM HEPES/KOH, pH 7.5, 100 mM KCl, and 5 mM $MgCl_2$) as described previously (29). The reaction was started by the addition of 1 mM ATP and terminated by the addition of 1 μM carbonyl cyanide *p*-trifluoromethoxyphenylhydrazone (FCCP). ATP synthesis activity was measured at 50 °C in PA4-buffer containing 1 mM ADP, 25 mM KPi, pH 7.5, and membrane vesicles (4.5 μg of protein/ml). Oxidized and reduced membrane vesicles were prepared by treating with 20 μM $CuCl_2$ for 30 min and 10 mM DTT for 30 min, respectively. EDTA (final concentration, 1 mM) was added to the oxidized vesicle solution prior to the assay of ATP synthesis to chelate free Cu^{2+}. EDTA was also added to the reduced vesicle solution to adjust the conditions. After a 5-min preincubation, the reaction was initiated by adding 5 mM NADH and terminated at 2, 4, 6, 8, 10, and 12 min by adding 2.5% trichloroacetic acid. The solution was neutralized to pH 7.7 with 0.25 M Tris acetate (pH 9.5), and the amount of synthesized ATP was determined with ATP bioluminescence assay kit CLSII (Roche Applied Science).

Other Assays—ATPase activity was monitored in triplicate in 50 mM HEPES/KOH, pH 7.5, containing 100 mM KCl, 5 mM $MgCl_2$, and 3 mM ATP with an ATP-regenerating system (31), and average hydrolysis rates in a time period from 3 to 6 min after initiation of the reactions at 40 °C were measured. The activity that hydrolyzed 1 μmol of ATP per minute was defined as one unit. 2′,3′-*O*-(2,4,6-trinitrophenyl)-ATP (TNP-ATP) and 2′,3′-*O*-(2,4,6-trinitrophenyl)-ADP (TNP-ADP) were purchased from Molecular Probes (Eugene, OR). Fluorescence change induced by the binding of TNP-nucleotide to the enzyme was monitored in a Spectrofluorometer model FP-6500 (Jasco, Tokyo, Japan) as performed previously (32). Protein concentrations were determined by using the BCA protein assay kit from Pierce, with bovine serum albumin as a standard.

RESULTS

Mutants—We generated three mutants. To obtain the enzyme with the up-fixed ε by cross-linking between γ and ε, one cysteine residue was introduced into the N-terminal region of the γ subunit (γS3C) and another was added to the C-terminal end of ε subunit (εCys^{134}) (Fig. 1*D*). To obtain the enzyme with the down-fixed ε by cross-linking two domains within ε, a mutant that had εA85C and εCys^{134} was used (Fig. 1*E*). To assess the relative population of enzymes with up- and down-state ε under various conditions, three mutations, γS3C, εA85C and εCys^{134} were introduced. The εAla^{85} is located in a region between two domains of ε and abuts on εCys^{134} (Cα distance is 9.0 Å) when the C-terminal domain adopts a hairpin structure (14). Therefore, εCys^{134} is expected to make the cross-link with γS3C when the ε is in the up-state or with εA85C when the ε is in the down-state (Fig. 1*F*). These mutations were termed $\gamma_c\epsilon_c$, ϵ_{cc}, and $\gamma_c\epsilon_{cc}$, respectively. The enzymes have one endogenous cysteine residue in the F_0a subunit. This cysteine is buried inside of the transmembrane region and does not respond to the $CuCl_2$ and 5,5′-dithiobis-(2-nitro)benzoic acid (DTNB) treatment employed in this report. The enzymes containing $\gamma_c\epsilon_c$, ϵ_{cc}, and $\gamma_c\epsilon_{cc}$ were as active as the wild-type enzyme in

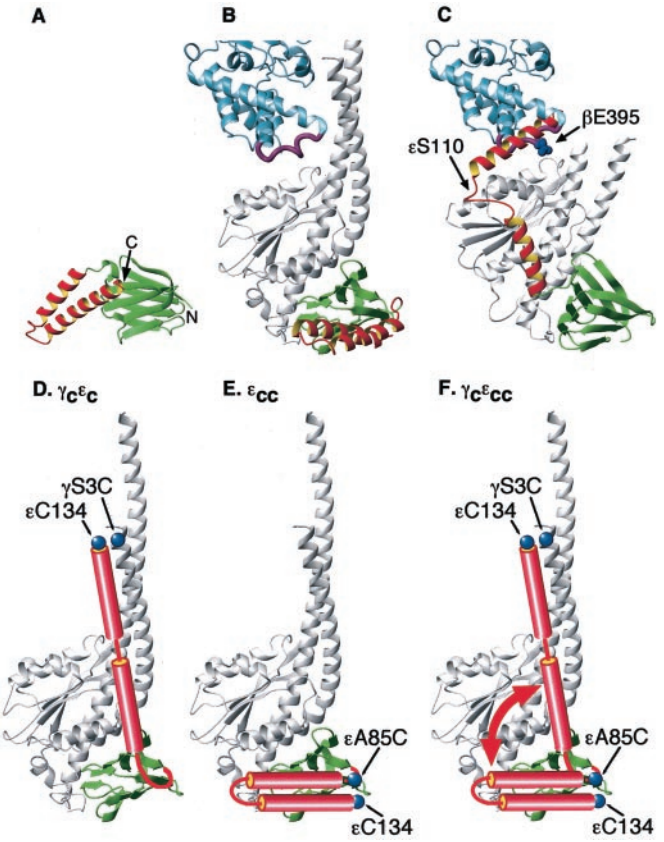

FIG. 1. **Conformations of the ϵ subunit.** *A*, crystal structure of the isolated *E. coli* ϵ subunit (16). N-terminal and C-terminal domains were shown with *green* and *red/yellow* colors, respectively. *B*, crystal structure of the down-state conformation of the δ subunit (equivalent to the ϵ subunit in bacterial F_1) observed in bovine mitochondrial F_1 (17). Only subunits of β_{TP}, γ, δ, and ϵ (no equivalent subunit in bacterial F_1) are depicted in the figure. A loop that contains a DELSEED sequence was colored *purple*. *C*, crystal structure of the γ′ϵ complex of *E. coli* F_1 (25) superimposed with the β_{TP} of bovine F_1. *Blue spheres* indicate βE395 residue of the DELSEED region (second Glu residue). Cα distance between βGlu^{381} and ϵSer^{108} is 24–27 Å, too far to be cross-linked. *D–F*, schematic diagrams of cross-link formation in $\gamma_c\epsilon_c$-F_1 (*D*), ϵ_{cc}-F_1 (*E*), and $\gamma_c\epsilon_{cc}$-F_1 (*F*). In the up-state, ϵCys^{134}-γS3C is to be cross-linked. In the down-state, ϵCys^{134}-ϵA85C is to be cross-linked. These figures were prepared by using a program package, MOLMOL (45). *ϵS110*, ϵSer^{110}; *βE395*, βGlu^{395}; *ϵC134*, ϵCys^{134}.

their reduced forms (Table I). Also ATPase activities of the inverted membrane vesicles prepared from the cells expressing the wild-type and the F_0F_1 mutants were similar to each other under the reducing conditions. SDS-PAGE analysis of the membrane vesicles showed almost identical band patterns for the three mutants and the wild-type (not shown). Therefore, the amounts of expressed mutant F_0F_1 in the inverted membranes are similar to that of the wild-type F_0F_1.

Cross-linking of ϵ in the Up-state—In the previous experiments using *E. coli* F_0F_1 (26), cysteine residues were introduced at positions γ99 and ϵ118 (*E. coli* numbering) to fix the conformation of ϵ in the up-state by a γ-ϵ cross-link. These positions were chosen based on the crystal structure of the γ′ϵ complex in which γ99 is located in the globular domain of γ′ and ϵ118 is in the extreme C-terminal helix of ϵ. In this structure, two helices do not fully extend but rather entwine the globular domain of γ′ (Fig. 1*C*). Expecting that helices of the up-state ϵ in the native enzyme could extend straighter, we introduced cysteine residues to a near N-terminal position of γ (γSer^3) atop the central helical coiled-coil of the γ subunit and to the C terminus of ϵ (ϵ134) (Fig. 1*D*). The membrane vesicles of *E. coli* expressing $\gamma_c\epsilon_c$-F_0F_1 were oxidized in 20 μM $CuCl_2$ for 20 min at 25 °C and analyzed with non-reducing SDS-PAGE (SDS-PAGE without prior reducing treatment) (Fig. 2*A*). Compared with a control $\gamma_c\epsilon_c$-F_0F_1, which was treated with 50 mM DTT prior to electrophoresis (Fig. 2*A*, *lane 1*), a new band appeared just below the band of the β subunit (Fig. 2*A*, *lane 4*, indicated by an *arrow*). Peptide sequencing of this band gave two kinds of amino acid sequences corresponding to the N terminus sequences of γ and ϵ, indicating that this band is a cross-link product of these two subunits. Consistently, band intensities of γ and ϵ decreased. The same γ-ϵ cross-link product was also readily generated in the purified $\gamma_c\epsilon_c$-F_1 under the same oxidizing conditions (Fig. 2*A*, *lane 5*). Cross-linking yields in the F_1 and F_0F_1 were estimated from the band intensities to be 80–85%. It is worth noting that γ-ϵ cross-link was generated spontaneously in ~40% of F_1 during the purification (2 days) that was carried out without DTT and EDTA. Also, ~60% of F_0F_1 in membrane vesicles were spontaneously oxidized during preparation. The efficient cross-linking between γS3C and ϵCys^{134} suggests that their proximal location is in the up-state conformation of ϵ in F_1 and F_0F_1 and that the C-terminal helix of ϵ inserts itself deep into the central cavity of the $\alpha_3\beta_3$. Because the isolated $\gamma_c\epsilon_c$-F_1 used in the above experiments was mostly free from endogenous nucleotide, the ϵ mostly adopts the up-state in the absence of bound nucleotides.

TABLE I
ATPase activity of the wild-type and mutant F_1 and F_0F_1

Enzymes[a]	ATPase activity[b]
	units/mg/min
Purified F_1	
Wild-type	10.6 ± 0.1
$\gamma_c\epsilon_c$	9.4 ± 0.1
$\gamma_c\epsilon_{cc}$	11.3 ± 0.5
ϵ_{cc}	9.9 ± 0.2
F_0F_1 (membrane vesicles)	
Wild-type	0.99 ± 0.02
$\gamma_c\epsilon_c$	0.89 ± 0.03
$\gamma_c\epsilon_{cc}$	1 ± 0.02
ϵ_{cc}	1 ± 0.1

[a] Reduced form of the enzymes was used for the analysis.
[b] ATPase activity was determined at 40 °C in the presence of 3 mM ATP. Values for F_0F_1 are the activity per 1 mg of membrane proteins.

Activities of F_1 and F_0F_1 with the Up-fixed ϵ—The ATPase activity of $\gamma_c\epsilon_c$-F_1 was severely inhibited by oxidation with its residual activity being only 21% of that of the reduced $\gamma_c\epsilon_c$-F_1, whereas the ATPase activity of the wild-type F_1 was hardly affected whether it was oxidized or reduced (Fig. 2*B*, *left panel*). The degree of inhibition by oxidation (79%) agreed well with the yield of cross-link by oxidation (81%). Similarly, the ATPase activity of the $\gamma_c\epsilon_c$-F_0F_1 contained in the vesicles was inhibited (77%) in proportion to the yield of cross-linking (80%) (Fig. 2*B*, *right panel*). Because ATP hydrolysis was blocked, oxidized $\gamma_c\epsilon_c$-F_0F_1 was unable to mediate ATP-driven proton translocation, whereas reduced $\gamma_c\epsilon_c$-F_0F_1 was fully capable of it (Fig. 2*C*). ATP synthesis activities of membrane vesicles containing reduced or oxidized $\gamma_c\epsilon_c$-F_0F_1 were also measured. Membrane vesicles containing the wild-type and $\gamma_c\epsilon_c$-F_0F_1 treated with DTT catalyzed ATP synthesis at 44.5 ± 2.8 and 34.7 ± 2.4 nmol of ATP/min/mg of membrane protein, respectively. Oxidized vesicles showed 71% (wild-type) and 75% ($\gamma_c\epsilon_c$-F_0F_1) of the ATP synthesis activity of the vesicles treated with DTT (Fig. 2*D*). Thus, ATP synthesis activity was retained after the formation of the γ-ϵ cross-link to lock the ϵ in the up-state. These results are consistent with the previous reports, demonstrating remarkable asymmetric inhibition by the up-state ϵ toward ATP hydrolysis (18, 26, 33).

Effect of ATP and ADP on the Conformational State of ϵ—To assess the distribution of the ϵ either in the up-state or down-

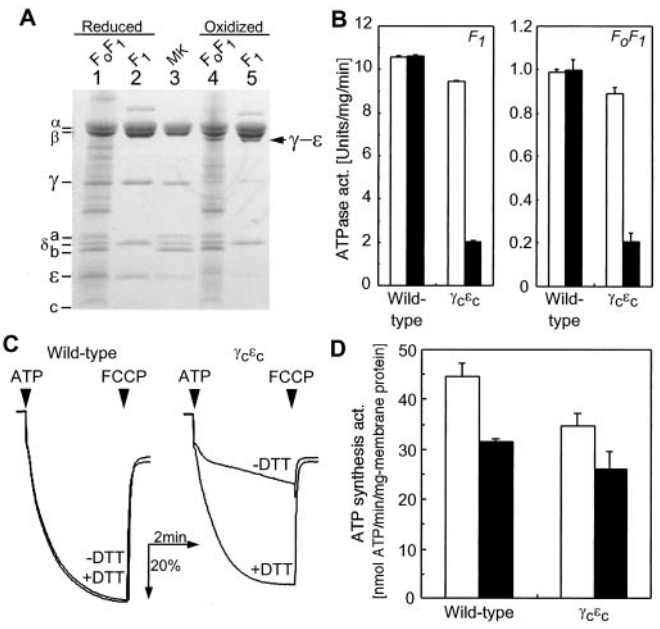

FIG. 2. **Cross-link between N terminus of the γ subunit and the C terminus of the ϵ subunit.** *A*, non-reducing SDS-PAGE analysis. *Lanes 1 and 4*, membrane vesicles containing $\gamma_c\epsilon_c$-F_0F_1; *lanes 2 and 5*, isolated $\gamma_c\epsilon_c$-F_1; *lane 3*, isolated wild-type F_0F_1 (*MK*). All samples except for *lane 3* were treated with 20 μM $CuCl_2$ for 30 min at 25 °C. Then, samples of *lanes 1* and 2 were reduced with 50 mM DTT for 1 h. A band of γ-ϵ cross-linked product appeared just below the band of the β subunit. *B*, effect of the γ-ϵ cross-linking on ATPase activities of the isolated $\gamma_c\epsilon_c$-F_1 (*left panel*) and membrane vesicles containing $\gamma_c\epsilon_c$-F_0F_1 (*right panel*). ATP hydrolysis by the reduced (*white bars*) and oxidized (*black bars*) $\gamma_c\epsilon_c$-F_1 and membrane vesicles containing $\gamma_c\epsilon_c$-F_0F_1 were assayed at 40 °C. The same procedures were applied to the wild-type F_1 and F_0F_1. *C*, effect of the γ-ϵ cross-linking on proton pump activity. Proton pump activities of the reduced or oxidized membrane vesicles were analyzed by monitoring the fluorescence of 9-amino-6-chloro-2-methoxyacridine at 40 °C. Prior to the analysis, 1 mM EDTA was added to the solutions to remove free Cu^{2+}. At the indicated times, pumping was initiated by adding 1 mM ATP and terminated by 1 μg/ml FCCP. *D*, effect of the γ-ϵ cross-linking on ATP synthesis activity. The reactions were started by addition of 5 mM NADH to the membrane vesicle solutions containing reduced or oxidized wild-type F_0F_1 and $\gamma_c\epsilon_c$-F_0F_1. The reactions were carried out at 50 °C, and the amount of generated ATP was measured with luciferase.

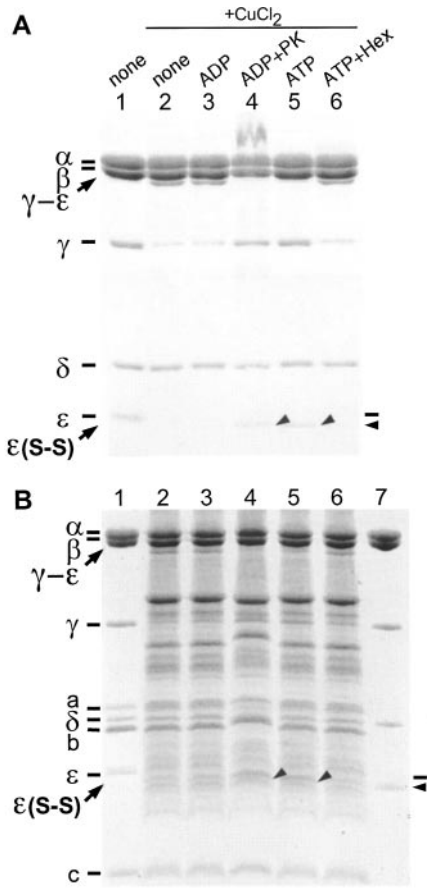

FIG. 3. **Effect of ATP and ADP on the conformational state of the ϵ subunit.** *A*, analysis of $\gamma_c\epsilon_{cc}$-F_1. $\gamma_c\epsilon_{cc}$-F_1 was incubated with indicated components for 2 min. Concentrations of ADP (*lanes 3 and 4*) and ATP (*lanes 5 and 6*) were 3 mM. For the sample of *lane 4*, 125 μg/ml pyruvate kinase and 9.4 mM phosphoenolpyruvate (final concentrations) were added and incubated for 1 min. For the sample of *lane 6*, 9.4 units/ml hexokinase and 38 mM glucose (final concentrations) were added and incubated for 1 min. The samples were reduced with 50 mM DTT (*lane 1*) or oxidized with 20 μM $CuCl_2$ (*lanes 2–6*) for 10 min and applied to non-reducing SDS-PAGE. *Lanes 1 and 2*, no nucleotide; *lane 3*, ADP; *lane 4*, ADP followed by pyruvate kinase treatment; *lane 5*, ATP; *lane 6*, ATP followed by hexokinase (*Hex*) treatment. *Arrowheads* in *lanes 4* and *5* indicate the position of the ϵ subunit with internal cross-link. All reactions were carried out in 50 mM HEPES/NaOH, pH 7.5, containing 100 mM NaCl and 5 mM $MgCl_2$ at 50 °C. A distorted band above of the α subunit band in *lane 4* was pyruvate kinase. *B*, analysis for $\gamma_c\epsilon_{cc}$-F_0F_1. Membrane vesicles containing $\gamma_c\epsilon_{cc}$-F_0F_1 were used for the analysis. *Lane 1*, reduced $\gamma_c\epsilon_{cc}$-F_0F_1, no nucleotide; *lanes 2–6*, membrane vesicles containing $\gamma_c\epsilon_{cc}$-F_0F_1 treated with the same procedures as for *panel A*; *lane 7*, $\gamma_c\epsilon_{cc}$-F_1 incubated with ATP (the same sample as in *panel A*, *lane 5*) to show the band position of the ϵ subunit with internal cross-link. The samples were reduced with 50 mM DTT (*lane 1*) or oxidized with 100 μM $CuCl_2$ (*lanes 2–6*) and applied to non-reducing SDS-PAGE.

state, $\gamma_c\epsilon_{cc}$-F_1 and $\gamma_c\epsilon_{cc}$-F_0F_1 were used. With oxidation procedures, the down-state ϵ can be detected as a band corresponding to an internally cross-linked ϵ (ϵA85C and ϵC^{134}) and the up-state ϵ as a γ-ϵ band (γS3C and ϵCys^{134}). The ϵ subunit behaved very similarly in $\gamma_c\epsilon_{cc}$-F_1 and $\gamma_c\epsilon_{cc}$-F_0F_1 (Fig. 3, *A* and *B*). In the absence of nucleotides, the ϵ in F_1 and in F_0F_1 was mostly in the up-state (Fig. 3, *A* and *B*, *lanes 2*), and the up-state conformation was stabilized when 3 mM ADP was present (Fig. 3, *A* and *B*, *lanes 3*).[2] The further addition of 5 mM P_i caused no significant change (not shown). However, the γ-ϵ band disappeared, and the internally cross-linked ϵ band (Fig. 3, *A* and *B*, *arrowheads*) appeared when ADP was converted into ATP by pyruvate kinase (Fig. 3, *A* and *B*, *lanes 4*). Also, the internally cross-linked ϵ band appeared when ATP was added from the beginning (Fig. 3, *A* and *B*, *lanes 5*). The addition of hexokinase and glucose to the sample of the *lanes 5* (Fig. 3, *A* and *B*) resulted in the appearance of the γ-ϵ band (Fig. 3, *A* and *B*, *lanes 6*). Thus, it is clear that the ϵ subunit in F_1 and F_0F_1 adopts reversibly the up-state conformation in the presence of ADP and the down-state conformation in the presence of ATP. As shown previously (19), hydrolysis of ATP is not necessary to stabilize the down-state ϵ, because 3 mM AMP-PNP also stabilized the down-state conformation of ϵ (not shown).

TNP-AT(D)P Binding to F_1 with Up- or Down-state ϵ—It has been known that a nucleotide analogue, TNP-AT(D)P, increases its fluorescence upon binding to F_1 (32). Taking advantage of this, we compared initial kinetics of nucleotide binding to the enzymes that contained the up- or down-state ϵ. To measure the binding to the nucleotide binding site with the highest affinity, a sub-stoichiometric amount of TNP-AT(D)P was mixed with $\gamma_c\epsilon_c$-F_1 or ϵ_{cc}-F_1, and fluorescence changes were monitored. Time courses of TNP-ADP binding were almost the

[2] We reported previously that ADP, though less effective than ATP, induced the down-state conformation of the ϵ subunit in the $\alpha_3\beta_3\gamma\epsilon$ complex (19). When we used ADP pretreated with hexokinase and glucose in the experiment, the down-state conformation was not detected. Therefore, contaminated ATP in the commercial ADP might be the reason for the previous result.

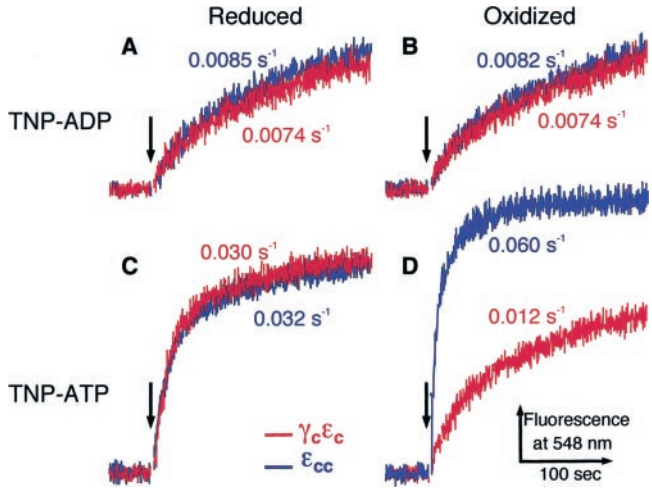

FIG. 4. **TNP-ATP binding to F_1 with the up- or down-fixed ϵ subunit.** To obtain F_1 with the up- or down-fixed ϵ subunit by γ-ϵ cross-linking ($\gamma_c\epsilon_c$-F_1) or internal cross-linking within ϵ (ϵ_{cc}-F_1), purified $\gamma_c\epsilon_c$-F_1 and ϵ_{cc}-F_1 in 50 mM HEPES/KOH, pH7.5, were oxidized with 20 μM ($\gamma_c\epsilon_c$-F_1) or 100 μM (ϵ_{cc}-F_1) $CuCl_2$ for 1 h at 25 °C. Reduced samples were not subjected to this oxidation procedures. TNP-AT(D)P (50 nM) was incubated at 50 °C for 5 min in 50 mM HEPES/KOH, pH 7.5, containing 100 mM KCl, 5 mM $MgCl_2$, and 20 μl of F_1 (6 μM) were added into the cuvette (final F_1 concentration, 100 nM) at the time indicated with *arrows* (final volume, 1.2 ml). Fluorescence change was monitored at 548 nm with an excitation light at 410 nm. *Red traces*, $\gamma_c\epsilon_c$-F_1; *blue traces*, ϵ_{cc}-F_1. Apparent rate constants for the nucleotide binding were estimated by fitting single exponential functions to the time courses, as shown.

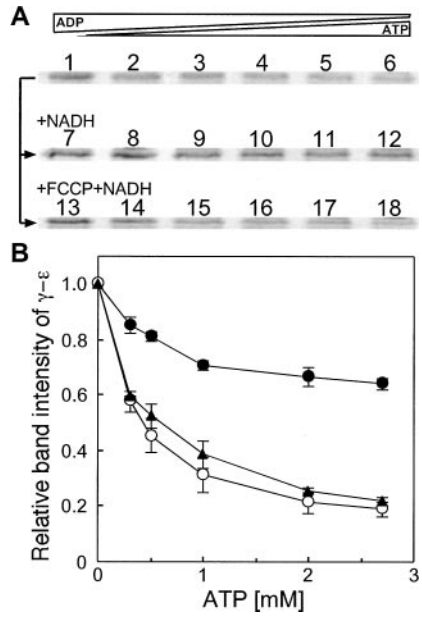

FIG. 5. **Effect of proton motive force on the conformational state of ϵ subunit in F_0F_1.** *A*, membrane vesicles containing $\gamma_c\epsilon_{cc}$-F_0F_1 were incubated for 3 min with mixtures of varying amounts of ATP and ADP (ATP + ADP = 3 mM). An aliquot of each reaction mixture was transferred to another tube, treated with 200 μM DTNB for 5 min to fix the conformational state of the ϵ subunit by cross-linking, and subjected to non-reducing SDS-PAGE analysis (*lanes 1–6*). For the remaining reaction mixtures, 5 mM NADH (*lanes 13–18*) or 5 mM NADH + 3 μg/ml FCCP (*lanes 6–12*) was added, and incubation was continued for 5 min. Then, the reaction mixtures were treated with 200 μM DTNB for 5 min and analyzed with non-reducing SDS-PAGE. DTNB was used instead of $CuCl_2$ as an oxidant, because DTNB is less harmful to the membrane vesicles than $CuCl_2$. Concentrations of ATP and ADP were as follows: 0 and 3 mM (*lanes 1*, *7*, and *13*); 0.3 and 2.7 mM (*lanes 2*, *8*, and *14*); 0.5 and 2.5 mM (*lanes 3, 9,* and *15*); 1 and 2 mM (*lanes 4, 10,* and *16*); 2 and 1 mM (*lanes 5, 11,* and *17*); and 2.7 and 0.3 mM (*lanes 6, 12,* and *18*), respectively. The experiments were carried out at 50 °C in 50 mM HEPES/NaOH, pH 7.5, containing 100 mM NaCl and 5 mM $MgCl_2$. It was confirmed that NADH oxidation by respiratory chains of vesicles under these conditions was as active as that at 37 °C and could generate proton motive force. In this figure, γ-ϵ bands formed by cross-linking are shown. *B*, the relative staining intensities of the γ-ϵ bands in *panel A* were plotted against the ATP concentrations. *Closed triangles*, the control samples (*lanes 1–6*); *closed circles*, NADH (*lanes 7–12*); *open circles*, NADH + FCCP (*lanes 13–18*).

same for $\gamma_c\epsilon_c$-F_1 and ϵ_{cc}-F_1, irrespective of whether they were reduced or oxidized (Fig. 4, *A* and *B*). The wild-type F_1, with or without oxidizing treatment, also showed the same kinetics of TNP-ADP binding (not shown). These results indicated that TNP-ADP binding to F_1 was not affected by the conformational states of the ϵ subunit. The time course of TNP-ATP binding to reduced $\gamma_c\epsilon_c$-F_1 was also the same as that of ϵ_{cc}-F_1 (Fig. 4*C*) and wild-type F_1 (not shown), ensuring no significant effect of the introduced cysteines on the TNP-ATP binding kinetics of F_1. The time course of TNP-ATP binding to the oxidized $\gamma_c\epsilon_c$-F_1 (Fig. 4*D*, *bottom curve*) was similar to that of TNP-ADP binding to the oxidized $\gamma_c\epsilon_c$-F_1, indicating that TNP-ATP and TNP-ADP bind to the same site of F_1 with the up-fixed ϵ. The oxidized ϵ_{cc}-F_1, on the contrary, bound TNP-ATP much faster, and the fluorescence reaches a higher magnitude than with the oxidized $\gamma_c\epsilon_c$-F_1. (Fig. 4*D*, *upper curve*). Thus, F_1 with the down-state ϵ binds TNP-ATP quickly, whereas F_1 with the up-state ϵ binds it slowly. Accordingly, results of TNP-ATP binding to the reduced $\gamma_c\epsilon_c$-F_1 and ϵ_{cc}-F_1 in Fig. 4*C* are well interpreted as a mixture of F_1s with the up- and down-state ϵ.

Effect of Proton Motive Force on the State of ϵ—The inverted membrane vesicles containing $\gamma_c\epsilon_{cc}$-F_0F_1 were incubated for 3 min in the varying amounts of ATP and ADP, and conformational states of the ϵ subunit were analyzed with non-reducing SDS-PAGE after fixing the conformation by cross-linking (Fig. 5A, *lanes 1–6*). As ATP increased and ADP decreased, intensity of the γ-ϵ band decreased, as is expected from the results mentioned above. However, when the incubation was continued for another 5 min after the addition of NADH to impose proton motive force, the intensity of the γ-ϵ band did not significantly decrease even at high ATP concentrations (Fig. 5*A*, *lanes 7–12*). When FCCP, an uncoupler that dissipates proton motive force, was added in addition to NADH, the intensity of the γ-ϵ band was decreased as ATP increased, similar to Fig. 5*A*, *lanes 1–6* (Fig. 5*A*, *lanes 13–18*). These results suggest that when proton motive force is provided, the ϵ subunit in F_0F_1 strongly favors the up-state conformation irrespective of ADP/ATP balance. In other words, proton motive force counteracts the effect of ATP in the conformational transition of the ϵ subunit.

DISCUSSION

C Terminus of the ϵ Subunit Reaches the Center of F_1—The questions listed in the Introduction were mostly answered by the present study. Concerning the first question (i), it becomes evident that C terminus of ϵ in the up-state is located near the N terminus of the γ subunit.[3] To reach this position, referring to the structure of mitochondrial F_1, the C-terminal helices of ϵ have to extend ~70 Å from the exit (ϵA85) of the N-terminal β sandwich domain. Considering the length of α-helix per residue (1.5 Å/residue) (34), a peptide stretch of 48 residues from ϵAla^{85} to ϵLys^{133} can extend by 72 Å as an α-helix or longer as two helices with a connecting segment. Previous cross-linking results of *E. coli* F_1 between βGlu^{381} and ϵSer^{108} (9, 20–22) are explained by this new arrangement rather than by the γ′ϵ

[3] Very recently, we have succeeded in determining crystal structure of an $\alpha_3\beta_3\gamma\epsilon$ complex of thermophilic F_1 (Y. Shirakihara, M. Yoshida, and T. Suzuki, unpublished results). In the structure, C-terminal helices of the ϵ subunit indeed extend straight, and the C terminus of the ϵ subunit is close to the N terminus of the γ subunit.

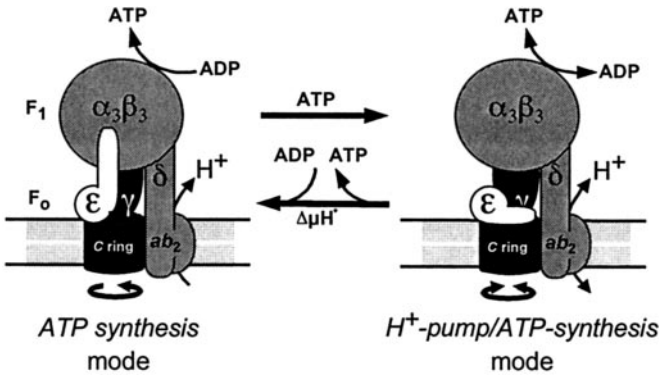

FIG. 6. **Schematic diagram of two forms of the F_0F_1 with up-state ϵ (*left*) and down-state ϵ (*right*).** The F_0F_1 with up-state ϵ can catalyze ATP synthesis but not ATP hydrolysis (ATP synthesis mode). This form is stabilized by ADP and proton motive force. The F_0F_1 with down-state ϵ can catalyze ATP synthesis as well as ATP hydrolysis (proton pump/ATP synthesis mode). This form is favored when ATP is present. Transition between two forms is determined by proton motive force and ADP/ATP balance.

structure (Fig. 1, compare *C* and *D*) (25). Probably, the γ′ϵ structure represents an intermediate conformation that appears during the transition of ϵ from the down-state to the up-state. Our study suggests that three helices, the coiled-coil of the γ subunit and C-terminal helix of the ϵ subunit, rather than two as previously thought, rotate as a body within the $\alpha_3\beta_3$ ring when F_0F_1 with the up-state ϵ is synthesizing ATP.

ATP and ADP Have Opposite Effects on the Conformational States of the ϵ Subunit—As to the second question (ii), it is now clear that the ϵ subunit, either in F_1 or F_0F_1, is in the up-state conformation in the absence of nucleotide or the presence of ADP and is in the down-state conformation in the presence of ATP. Thus, ATP and ADP counteract each other (Fig. 6). Reciprocally, an ATP analogue, TNP-ATP, binds quickly to F_1 with down-state ϵ but slowly to F_1 with up-state ϵ. An ADP analogue, TNP-ADP, does not show binding preference between F_1s with up- and down-state ϵ. Therefore, if TNP-AT(D)P mimics the AT(D)P correctly in binding to F_1, the answer to the third question (iii) will be that F_1s with down-state ϵ indeed prefer ATP to ADP, whereas F_1s with up-state ϵ bind both ATP and ADP in the same slow kinetics. The results are consistent with the previous observation that the $\alpha_3\beta_3\gamma$ complex binds TNP-ATP quickly, but the reconstituted $\alpha_3\beta_3\gamma\epsilon$ complex does this slowly (32), because without previous exposure to nucleotide, the ϵ subunit in the reconstituted $\alpha_3\beta_3\gamma\epsilon$ must be in the up-state.

The ϵ Subunit Transits between Two States Depending on Proton Motive Force and ADP/ATP—This study has revealed that proton motive force counteracts the effect of ATP by stabilizing the up-state ϵ (answer to the fourth question (iv)). Therefore, the two conformational states of ϵ in F_0F_1 are alternated by two factors, *i.e.* proton motive force and ADP/ATP balance (Fig. 6). At high proton motive force and low ATP, ϵ is predominantly in the up-state, and F_0F_1 is geared to the ATP synthesis mode. At low proton motive force and high ATP, ϵ adopts the down-state and F_0F_1 hydrolyzes ATP to pump out protons, generating proton motive force with enough magnitude to drive uptake of nutrients and flagella motion.

Role of C-terminal Helices of the ϵ Subunit—In some bacteria, such as *Chlorobium limicola* (35) and *Thermotoga neapolitana* (36), the native ϵ subunit lacks the C-terminal helical domain. Without the C-terminal helical domain, the ϵ subunit cannot adopt the up-state arrangement and should be always in the state that is functionally similar to the down-state. These bacteria grow in anaerobic environments, and F_0F_1 should work as an ATP hydrolysis-driven proton pump. Because the F_0F_1 with up-state ϵ is unable to mediate ATP hydrolysis-driven proton pumping, these bacteria do not need, or even had better delete, the C-terminal domain of the ϵ subunit. F_0F_1 with down-state ϵ can catalyze both ATP synthesis and ATP hydrolysis (26). Therefore, it is not surprising that a mutant *E. coli* F_0F_1 containing the ϵ subunit with deleted C-terminal helical domain or an artificially fused protein at the C terminus can support aerobic growth by oxidative phosphorylation (37, 38). A similar observation was reported recently for chloroplast F_0F_1 (33). Then, a critical question should be asked, *i.e.* what is the essential function of the F_0F_1 whose ϵ subunit is in the up-state? Probably, the F_0F_1 with the up-state ϵ plays an important role under starving conditions rather than in rich nutritional environments. In *E. coli* cells, total concentration of cellular adenine nucleotides is maintained to be ~3 mM (39), but the fraction of ATP in total adenine nucleotide pool varies from 3 to 0.3 mM in parallel with growth rate (40–42) through ribosome synthesis (43) and transcription (44). As ATP concentration decreases from 3 to 0.3 mM in the absence of proton motive force, the population of the F_0F_1 with up-state ϵ increases about 3-fold (Fig. 5*B*) so that hydrolysis of the precious ATP by F_0F_1 is suppressed. For any organisms, regulation of ATP synthesis/hydrolysis to meet physiological demand in quickly changing nutritional conditions is a critical matter, and conformational transition of the ϵ subunit in F_0F_1 might constitute a part of an elaborately integrated regulatory system that awaits further study.

Acknowledgments—We thank our colleagues, Drs. H. Ueno, N. Mitome, T. Hisabori, and T. Mogi, for helpful discussions. Analytical condition for ATP synthesis activity was optimized by the assistance of N. Mitome.

REFERENCES

1. Boyer, P. D. (1997) *Annu. Rev. Biochem.* **66,** 717–749
2. Yoshida, M., Muneyuki, E., and Hisabori, T. (2001) *Nat. Rev. Mol. Cell Biol.* **2,** 669–677
3. Pedersen, P. L. (2002) *J. Bioenerg. Biomembr.* **34,** 327–332
4. Capaldi, R. A., and Aggeler, R. (2002) *Trends Biochem. Sci.* **27,** 154–160
5. Senior, A. E., Nadanaciva, S., and Weber, J. (2002) *Biochim. Biophys. Acta* **1553,** 188–211
6. Duncan, T. M., Bulygin, V. V., Zhou, Y., Hutcheon, M. L., and Cross, R. L. (1995) *Proc. Natl. Acad. Sci. U. S. A.* **92,** 10964–10968
7. Noji, H., Yasuda, R., Yoshida, M., and Kinosita, K., Jr. (1997) *Nature* **386,** 299–302
8. Ren, H., and Allison, W. S. (2000) *Biochim. Biophys. Acta* **1458,** 221–233
9. Aggeler, R., Ogilvie, I., and Capaldi, R. A. (1997) *J. Biol. Chem.* **272,** 19621–19624
10. Schulenberg, B., Wellmer, F., Lill, H., Junge, W., and Engelbrecht, S. (1997) *Eur. J. Biochem.* **249,** 134–141
11. Fillingame, R. H., and Dmitriev, O. Y. (2002) *Biochim. Biophys. Acta* **1565,** 232–245
12. Laget, P. P., and Smith, J. B. (1979) *Arch. Biochem. Biophys.* **197,** 83–89
13. Sternweis, P. C., and Smith, J. B. (1980) *Biochemistry* **19,** 526–531
14. Uhlin, U., Cox, G. B., and Guss, J. M. (1997) *Structure* **5,** 1219–1230
15. Wilkens, S., Dahlquist, F. W., McIntosh, L. P., Donaldson, L. W., and Capaldi, R. A. (1995) *Nat. Struct. Biol.* **2,** 961–967
16. Wilkens, S., and Capaldi, R. A. (1998) *J. Biol. Chem.* **273,** 26645–26651
17. Gibbons, C., Montgomery, M. G., Leslie, A. G. W., and Walker, J. E. (2000) *Nat. Struct. Biol.* **7,** 1055–1061
18. Schulenberg, B., and Capaldi, R. A. (1999) *J. Biol. Chem.* **274,** 28351–28355
19. Kato-Yamada, Y., Yoshida, M., and Hisabori, T. (2000) *J. Biol. Chem.* **275,** 35746–35750
20. Aggeler, R., and Capaldi, R. A. (1996) *J. Biol. Chem.* **271,** 13888–13891
21. Aggeler, R., Chicas-Cruz, K., Cai, S. X., Keana, J. F. W., and Capaldi, R. A. (1992) *Biochemistry* **31,** 312956–312961
22. Grüber, G., and Capaldi, R. A. (1996) *J. Biol. Chem.* **271,** 32623–32628
23. Hara, K. Y., Kato-Yamada, Y., Kikuchi, Y., Hisabori, T., and Yoshida, M. (2001) *J. Biol. Chem.* **276,** 23969–23973
24. Komatsu-Takaki, M. (1993) *Eur. J. Biochem.* **214,** 587–591
25. Rodgers, A. J., and Wilce, M. C. (2000) *Nat. Struct. Biol.* **7,** 1051–1054
26. Tsunoda, S. P., Rodgers, A. J. W., Aggeler, R., Wilce, M. C. J., Yoshida, M., and Capaldi, R. A. (2001) *Proc. Natl. Acad. Sci. U. S. A.* **98,** 6560–6564
27. Hausrath, A. C., Capaldi, R. A., and Matthews, B. W. (2001) *J. Biol. Chem.* **276,** 47227–47232
28. Aggeler, R., Haughton, M. A., and Capaldi, R. A. (1995) *J. Biol. Chem.* **270,** 9185–9191
29. Suzuki, T., Ueno, H., Mitome, N., Suzuki, J., and Yoshida, M. (2002) *J. Biol. Chem.* **277,** 13281–13285
30. Landt, O., Grunert, H. P., and Hahn, U. (1990) *Gene* **96,** 125–128

31. Suzuki, T., Suzuki, J., Mitome, N., Ueno, H., and Yoshida, M. (2000) *J. Biol. Chem.* **275,** 37902–37906
32. Kato, Y., Matsui, T., Tanaka, N., Muneyuki, E., Hisabori, T., and Yoshida, M. (1997) *J. Biol. Chem.* **272,** 24906–24912
33. Nowak, K. F., Tabidze, V., and McCarty, R. E. (2002) *Biochemistry* **41,** 15130–15134
34. Dunn, S. D., McLachlin, D. T., and Revington, M. (2000) *Biochim. Biophys. Acta* **1458,** 356–363
35. Xie, D., Lill, H., Hauska, G., Maeda, M., Futai, M., and Nelson, N. (1993) *Biochim. Biophys. Acta* **1172,** 267–273
36. Iida, T., Inatomi, K., Kamagata, Y., and Maruyama, T. (2002) *Extremophiles* **6,** 369–375
37. Kuki, M., Noumi, T., Maeda, M., Amemura, A., and Futai, M. (1988) *J. Biol. Chem.* **263,** 17437–17442
38. Cipriano, D. J., Bi, Y., and Dunn, S. D. (2002) *J. Biol. Chem.* **277,** 16782–16790
39. Neuhard, J., and Nygaard, P. (1987) in *Escherichia coli and Salmonella typhimurium: Cellular and Molecular Biology* (Neidhardt, F. C., ed) 1st Ed., pp. 445–473, ASM Press, Washington, D. C.
40. Franzen, J. S., and Binkley, S. B. (1961) *J. Biol. Chem.* **236,** 515–519
41. Smith, R. C., and Maaløe, O. (1964) *Biochim. Biophys. Acta* **86,** 229–234
42. Bagnara, A. S., and Finch, L. R. (1973) *Eur. J. Biochem.* **36,** 422–427
43. Gaal, T., Bartlett, M. S., Ross, W., Turnbough, C. L., Jr., and Gourse, R. L. (1997) *Science* **278,** 2092–2097
44. Alper, S., Dufour, A., Garsin, D. A., Duncan, L., and Losick, R. (1996) *J. Mol. Biol.* **260,** 165–177
45. Koradi, R., Billerter, M., and Wuthrich, K. (1996) *J. Mol. Graphics* **14,** 51–55